PLOS CLIMATE

Contrasting current and future surface melt rates on the ice sheets of Greenland and Antarctica: Lessons from in situ observations and climate models

Michiel R. van den Broeke ⓘ *, **Peter Kuipers Munneke, Brice Noël, Carleen Reijmer** ⓘ, **Paul Smeets, Willem Jan van de Berg** ⓘ, **J. Melchior van Wessem**

Institute for Marine and Atmospheric Research Utrecht, Utrecht University, Utrecht, The Netherlands

* m.r.vandenbroeke@uu.nl

Check for updates

🔓 OPEN ACCESS

Abstract

Surface meltwater production impacts the mass balance of the Greenland and Antarctic ice sheets in several ways, both directly (e.g., through runoff in Greenland) and indirectly (e.g., through cryo-hydrologic warming and frontal melt of marine-terminating glaciers in Greenland and hydrofracturing of ice shelves in Antarctica). Despite its importance, the spatial and temporal patterns in melt rates on both ice sheets are still relatively poorly understood. In this contribution we review and contrast surface melt 'weather '(i.e., short term, intra- and interdiurnal variability) and surface melt 'climate' (i.e., longer term, interannual variability and future melt) of both ice sheets. We find that in situ observations using suitably equipped (automatic or staffed) weather stations are invaluable for a complete understanding of the melt process, which represents the complex transport of energy by radiation, turbulence, and molecular conduction between the lower atmosphere, the ice/snow surface, and the subsurface ice/snow layers. We provide example time series of ice sheet melt 'weather' for the marginal Greenland ice sheet, where warm and humid air masses tend to increase surface melt rate, and for coastal East Antarctica, where the opposite happens. Apart from process understanding, these in situ observations, which especially in Antarctica are scarce in space and time, are also invaluable to validate, evaluate and calibrate satellite- and model-based estimates of ice sheet surface melt rate. We provide examples of modelled melt maps for both ice sheets, and melt projections for a high-warming, fossil-fuelled development scenario. Although important milestones in melt observations (both in-situ and remotely sensed) and melt models (both global and regional) have recently been reached, we identify multiple outstanding research questions pertaining to current and future ice sheet surface melt rates.

1. Introduction

Satellite and in situ observations show that the ice sheets of Greenland (GrIS) and Antarctica (AIS) are losing mass at increasing rates [1, 2], contributing to the recent acceleration in sea

level rise [3, 4]. Ice sheet mass loss broadly consists of i) surface processes, ii) basal melt of grounded and iii) floating ice, and iv) iceberg calving. However, quantifying each of these components individually is challenging and requires information from climate models, because many processes are involved, and each ice sheet has its own climatic setting. The dominant process responsible for contemporary GrIS mass loss is increased melt at the ice sheet surface and subsequent supraglacial/subglacial meltwater runoff, especially since the mid 1990s [5]. Recent observations confirm an expansion of the area from which runoff occurs [6, 7]. Along its margins, the GrIS has a well-defined ablation zone, where relatively dark, semi-impermeable bare ice is exposed at the surface in summer, strongly enhancing melt and runoff [8, 9]. Fig 1A shows the typical ablation zone icescape along the K-transect in the southwestern ice sheet, a region with one of the highest annual melt rates on the GrIS [10]. Apart from directly leading to mass loss through runoff, meltwater produced at the ice sheet surface also has the potential to influence ice flow. Meltwater that reaches the ice sheet–bedrock interface through moulins (vertical meltwater channels) and crevasses, can temporarily accelerate ice flow through basal lubrication [11–13] and/or soften the ice through cryo-hydrologic warming [14]. When fresh meltwater subsequently enters the saline fjords at the grounding line of marine terminating glaciers, it rises to the surface, enhancing turbulent mixing and frontal melting [15, 16]. As a result, outlet glaciers have accelerated and solid ice discharge has increased, especially since ~2000, further adding to GrIS mass loss [17, 18].

Contemporary AIS mass loss occurs in the Antarctic Peninsula (AP) and coastal East and West Antarctica but is concentrated in the Amundsen and Bellingshausen Sea sectors of West Antarctica. Here, warm ocean waters melt and thin ice shelves from below, leading to damage and weakening [21], reduced buttressing and increased ice discharge, notably since the mid 1990s [22]. In the cold Antarctic climate, surface melt is mostly intermittent, except in the AP with its relatively mild summers [23, 24]. A well-defined ablation zone is absent on the contiguous AIS, apart from scattered blue ice areas formed by wind-driven snow erosion and sublimation, which cover 1–2% of the ice sheet surface [25]. Owing to their lower albedo (0.55 vs. >0.8 for clean snow), blue ice areas show locally enhanced surface melt rates [26–30]. The remainder of the ice sheet surface, including its floating ice shelves, is covered by a layer of compressed snow, called firn, that is up to 120 m thick [31]. Fig 1B shows the surface of

Fig 1. A: Automatic weather station S5 along the K-transect in the lower ablation zone of the south-western GrIS in September 2014 (67°06'N, 50°07'W, ~500 m asl, credit Christian Steger, IMAU) [19] and B: meteorological measurement site of Neumayer base in austral summer 2004/05, situated on the Ekström ice shelf in East Antarctica (70°39'S, 8°15'W, ~50 m asl, credit Bernd Loose, Alfred-Wegener-Institut für Polar- und Meeresforschung) [20]. Both stations are situated near the ice sheet margin, which for the GrIS in this sector is land-terminating, whereas it is marine terminating at Neumayer.

https://doi.org/10.1371/journal.pclm.0000203.g001

Ekström ice shelf in East Antarctica, on which the German research base Neumayer is situated. Neumayer is one of the few Baseline Surface Radiation Network (BSRN) stations in Antarctica and the station with the longest high-quality observational surface radiation record on the AIS [20, 32]. Integrated over the AIS, almost all surface meltwater is refrozen in the cold firn, limiting runoff [33]. As a result, surface melt mostly plays an indirect role in AIS mass loss. When the firn layer is saturated, additional meltwater can form melt ponds which act as precursors to ice shelf disintegration through hydrofracturing [34–37] in combination with plate bending and ocean swell often caused by atmospheric river activity [38–40]. Once the buttressing effect of ice shelves is removed, their tributary glaciers flow faster into the ocean, leading to grounded ice sheet mass loss and sea level rise [41–43]. This process is currently ongoing in the AP, where in recent decades a significant fraction of ice shelves has (partly) disintegrated, such as the Larsen A and Larsen B ice shelves in 1995 and 2002, respectively [44–46]. There are concerns that future warming will cause more ice shelves to disintegrate in the AP, but also elsewhere in Antarctica, leading to accelerations in AIS mass loss and sea level rise [47, 48]. From that perspective, the final break-up of Conger ice shelf in East Antarctica in 2022 is regarded a worrisome development.
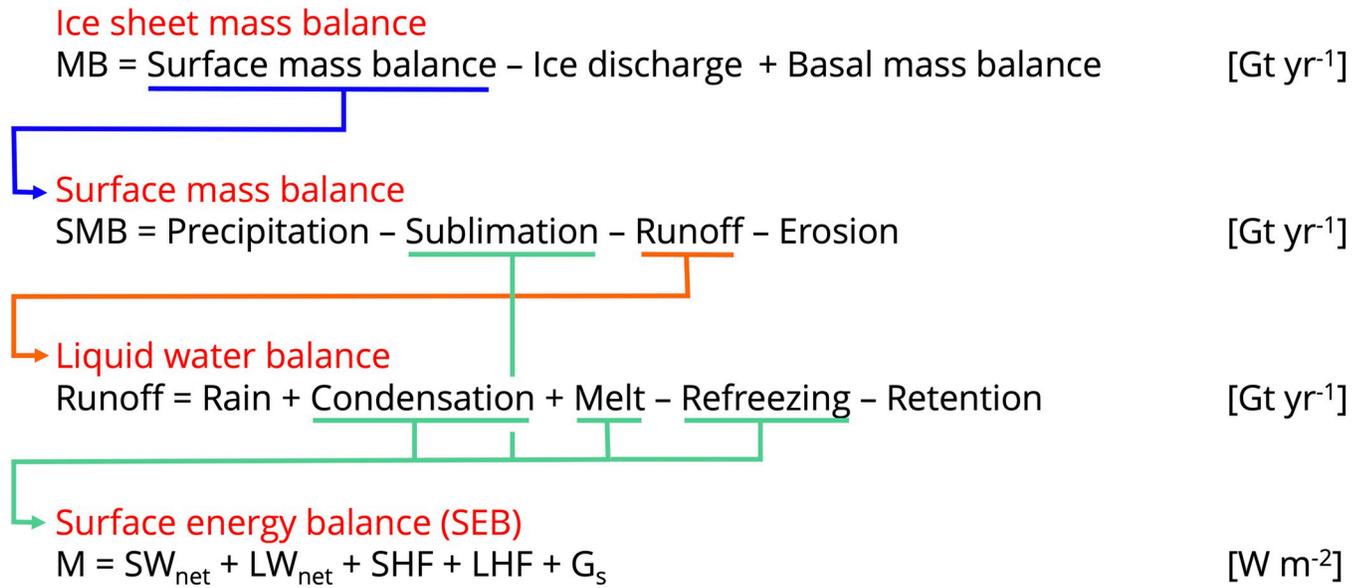
An alternative way for surface meltwater to be stored in ice sheets is in subsurface firn aquifers, which have been observed and modelled in the south-eastern, southern and north-western GrIS [49, 50], and on the AIS in the north-western AP [51–53] and on Wilkins ice shelf [54]. Observations show an increasing firn aquifer extent in the south-eastern GrIS [55], but time series are currently too short to confirm similar trends elsewhere on the GrIS or on the AIS. It is presently unknown whether firn aquifers impact AIS ice shelf viability, but their presence at the grounding line appears to be mutually exclusive with the presence of ice shelves, which implies that aquifers could also induce hydrofracturing, e.g., by year-round slowly releasing water to ice shelves or glaciers that feed them [56].

In summary, surface meltwater production is important for contemporary and future ice sheet mass balance. The main purpose of this review is to highlight and contrast the surface melt 'weather' and 'climate' of the GrIS and AIS. In Section 2 we discuss surface melt in the context of ice sheet mass balance and methods to quantify it. In Section 3 we discuss contemporary and projected future melt on the GrIS and AIS, followed by conclusions and an outlook in Section 4.

2. Methods to determine ice sheet surface melt rate

2.1 Definitions

Via the surface energy balance, liquid water balance and the surface mass balance, surface melting plays an intricate role in the ice sheet mass balance (Fig 2) [57]. The melt rate of ice and snow is determined by the melt energy flux (M, W m^{-2}), which becomes positive when the ice/snow surface reaches the melting point. Its magnitude is determined by the other components of the surface energy balance (SEB), the sum of all energy fluxes directed towards (defined positive) and away (negative) from the surface. Quantifying M thus requires knowledge of the surface fluxes of net shortwave radiation (SW_{net}), net longwave radiation (LW_{net}), turbulent sensible heat (SHF), turbulent latent heat (LHF) and conductive subsurface heat (G_s). This definition treats the surface as an infinitesimally thin layer without heat capacity; it also neglects the heat added to/extracted from the surface by precipitation as well as the penetration of shortwave radiation, which adds heat below the surface. In the near-absence of direct precipitation observations over the ice sheets, the former is difficult to quantify but assumed to be small in the current climate, even in regions with significant rainfall on ice, e.g., the south and north-west margins of the GrIS [58–60] and the north of the AP [61]. Penetration of

Ice sheet mass balance
MB = Surface mass balance – Ice discharge + Basal mass balance $\quad$ [Gt yr^{-1}]

Surface mass balance
SMB = Precipitation – Sublimation – Runoff – Erosion $\quad$ [Gt yr^{-1}]

Liquid water balance
Runoff = Rain + Condensation + Melt – Refreezing – Retention $\quad$ [Gt yr^{-1}]

Surface energy balance (SEB)
$M = SW_{net} + LW_{net} + SHF + LHF + G_s$ $\quad$ [W m^{-2}]

Fig 2. Definitions of ice sheet mass balance (MB), surface mass balance (SMB) and liquid water balance, all ice-sheet integrated mass fluxes expressed in gigatonnes per year (Gt yr^{-1}). 'Basal mass balance' refers to ablation at the ice-bedrock interface. 'Erosion' refers to removal of snow by wind, 'Retention' to the irreducible water content of porous snow. Note that the definition of SMB used here includes processes in the firn layer, and is formally referred to as 'climatic mass balance' [64]. Surface Energy Balance (SEB) is defined locally and expressed in watts per square metre (W m^{-2}). SEB symbols are explained in the main text. Adapted from [65].

https://doi.org/10.1371/journal.pclm.0000203.g002

shortwave radiation below the snow/ice surface is important for a correct prediction of subsurface snow/ice temperatures [62] and subsurface melt, but does not strongly affect total melt rate [63]. These assumptions are therefore maintained here.

2.2 In situ observations

To assess in-situ melt rate from near-surface meteorological data, the SEB equation is rewritten in terms of, and iteratively solved for, surface temperature T_s. Doing this in a physically consistent way requires near-surface observations of short- and longwave radiation, air temperature, humidity, wind speed and air pressure. Especially on the GrIS, substantial efforts have been made in setting up and maintaining long-term networks of 'SEB enabled' automatic weather stations (AWS); these AWS are equipped with radiation and other meteorological sensors that enable SEB closure and melt rate calculation, e.g. the K-transect, GC-Net and PROMICE [19, 66, 67]. The K-transect has been maintained by Utrecht University since 1990, the latter two networks have been merged in 2021 by the Geological Survey of Denmark and Greenland (GEUS). On the AIS, although the absolute number of AWS with ~150 is substantial [68], the number of such SEB-enabled AWS in melt regions remains small (< 20) and is only slowly increasing [24, 69]. When available, near-surface meteorological observations are subjected to correction and homogenization to reduce first-order measurement errors, for instance associated with riming and/or station tilt affecting the measurement of shortwave radiation [19, 66, 70, 71]. Validity of surface layer similarity is usually assumed in combination with a bulk gradient approach to quantify the turbulent fluxes, SHF and LHF, which requires assumptions about the surface aerodynamic roughness length [72]. Although over both ice sheets the surface aerodynamic roughness length can differ by several orders of magnitude in space and time [73–75], its value is usually prescribed as constant or used as tuning parameter [32]. Subsurface snow/ice density is prescribed or allowed to evolve to calculate G_s. If T_s exceeds the melting point of ice, it is reset to that value and the excess energy is assigned to melt energy M.

Evaluation of the calculated in-situ melt rate is essential. When the density of the melting material is known to a good approximation (e.g., glacier ice with a density of app. 917 kg m^{-3}), surface melt rate is directly observable as a surface height change, which can be used to evaluate modelled melt rate [76]. For all other cases, calculated T_s should be evaluated. Conveniently, down- and upward radiation fluxes are usually measured separately, so that LW_{down} can be used to close the SEB, while LW_{up} is used to estimate observed T_s (usually assuming unit surface emissivity). The root-mean-square-error between observed and modelled hourly T_s typically ranges between 0.6 and 2.0 K on the AIS [32, 77] and 1.0 to 1.5 K on the GrIS [10, 76]. Recently, the validity of the SEB closure assumption to calculate melt has been questioned for the GrIS percolation zone [78] where the skin layer formulation led to an apparent systematic overestimation of snowmelt by up to a factor of three. Other sources of uncertainty are processes that are neglected in most studies, e.g., the subsurface penetration of solar radiation and heat added by rain (see Section 2.1). Finally, it remains an interesting analytical problem to assign contributions from individual (positive and negative) SEB components to the melt energy, as only their sum counts for the melt rate.

2.3 Satellite remote sensing

Significant progress has recently been made in quantifying GrIS melt rate from space at (sub-) seasonal temporal resolution. Combining brightness temperature from the Special Sensor Microwave Imager/Sounder (SSMIS) with neural networks, trained by the excellent availability of in situ observations from AWS, resulted in a daily melt product with a horizontal resolution of ~3–6 km and 9 mm per day RMSE [79]. After applying a correction for the emergence velocity of the ice in the GrIS ablation zone, where upward ice flow compensates for the surface ablation, [80] could estimate 2011–2020 annual GrIS runoff using satellite altimetry from CryoSat-2 by quantifying the residual volume loss over summer. Using brightness temperatures from the ESA SMOS satellite [81] developed an L-band passive microwave algorithm to retrieve total snow liquid water and snow and firn density over the GrIS. The results qualitatively agree with model estimates of meltwater production. Previously for the AIS, [23, 82] used seasonally accumulated melting 'decibel days' from QuikSCAT, again calibrated using AWS-derived melt rates, to retrieve 1999–2009 seasonal total melt fluxes for the AIS. In a recent review, [83] discusses opportunities and problems in using a wide range of satellite products to assess AIS surface melt from space. Using liquid water detected by two active microwave sensors, a passive microwave sensor and an optical sensor, they found large differences between the various products, notably in blue ice areas, in aquifer regions in the AP, and during wintertime surface melt events.

2.4 Global and regional climate models

Until recently, most global climate (or earth system) models were run at too low spatial resolution (~100 km) and included too simplified snow cover/firn parametrizations to robustly quantify ice sheet surface melt rates. These shortcomings are gradually being addressed. For example, in the case of the Community Earth System Model version 2 (CESM2) [84], several improvements were made: a regional grid refinement over the GrIS was implemented [85], the representation of the firn layer was improved [86], a statistical downscaling was implemented based on elevation classes, and state of the art spectral snow albedo and snow microphysical schemes were included in the land model [87, 88]. These changes much improved the modelled GrIS melt fluxes [89]. Some problems remained for the AIS [90], but similar model upgrades, specifically new cloud microphysical parameterizations and an improved snow model, also have led to improvements there [91].

Given the large computational expense involved in running global coupled climate models, it is not expected that within the next decade these global models will operate over the ice sheets at resolutions required to resolve the large observed melt gradients. Until they do, resolution and physical parametrization issues can be addressed by using dedicated polar regional atmospheric climate models (RCMs, e.g., MAR, HIRHAM and RACMO), that run at higher (2.5–25 km) horizontal resolution over the ice sheets and their immediate surroundings. Polar RCMs also have improved representation of snow and ice processes and are forced at the lateral and top boundaries by atmospheric reanalysis products and/or earth system models, enabling the study of contemporary and future ice sheet surface melt weather and climate. For the GrIS, these models generally produce acceptable agreement with in-situ and spaceborne surface mass balance observations and each other, although regional differences remain and a detailed comparison of melt rates among models must still be made [57, 92]. For the AIS, uncertainties remain larger, with considerable model biases when compared to scarce in situ melt observations [24] and up to one order of magnitude melt differences (100–1000 Gt yr^{-1}) between RCMs. These differences can be traced back to differences in the treatment of snow accumulation (e.g., clouds, drifting snow sublimation) and meltwater (e.g., albedo, percolation, refreezing) [93–96]. Further model selection and development is hampered by a general scarcity of independent, in-situ and remotely sensed surface melt rate estimates over the AIS.

3. Ice sheet surface melt weather and climate

3.1 Intra- and interdiurnal variability

Fig 3 shows time series of hourly (near-)surface meteorological variables: 10 m wind speed (V_{10m}), 2 m air temperature (T_{2m}), surface temperature (T_s) and SEB components at AWS S5 (GrIS) and Neumayer base (AIS) (see Figs 1 and 4 for site specifics). The time series cover two months that mark the end of an arbitrary melt season (10 August– 9 October 2006 at S5 and 15 December 2004–14 February 2005 at Neumayer) and demonstrate the complex 'melt weather' arising from large intra- and interdiurnal variability in SEB. The two sites are broadly representative for the melt climates of the two ice sheet margins. The most conspicuous difference in the time series is that atmospheric temperature is mostly positive and surface melt is quasi-continuous at S5 (T_s = 0–˚C and M > 0 in Fig 3A), whereas the air temperature remains close to or below the melting point at Neumayer, where melt is intermittent and ceases during the brief polar night (Fig 3B). This has important implications for the magnitude of peak melt events. Once the surface reaches the melting point, it cannot further increase its temperature/specific humidity (being saturated at 0˚C), resulting in strong surface-to-air gradients in temperature and moisture when warm and moist air masses are advected over the ice sheet surface. If near-surface wind speeds are sufficiently high, the static stability of the atmospheric surface layer is overcome by wind shear, enabling strong turbulence despite the strong stratification. In the marginal western GrIS, this happens during so-called barrier wind events, during which high wind speed, temperature and cloud cover lead to large positive values of SHF and LHF [97]. At the same time, the clouds and high temperature and humidity of the air masses limit longwave heat loss, and in some cases LW$_{net}$ even turns positive. These increases in surface energy more than offset the reduction in SW$_{net}$ owing to clouds, resulting in very high melt rates. In Fig 3A, such a high-melt episode occurs between 14 and 20 August 2006 (grey band), resulting in hourly peak values of M > 500 W m^{-2} during the highest wind speed and temperatures. Under anticyclonic, clear sky conditions, wind speed, temperatures and melt flux are all significantly lower. This confirms that at the GrIS margin, interdiurnal melt variability (melt 'weather') is mostly explained by synoptic systems and the associated increases in SHF, LHF and LW$_{net}$ [76]. The relative importance of solar radiation absorption for melting
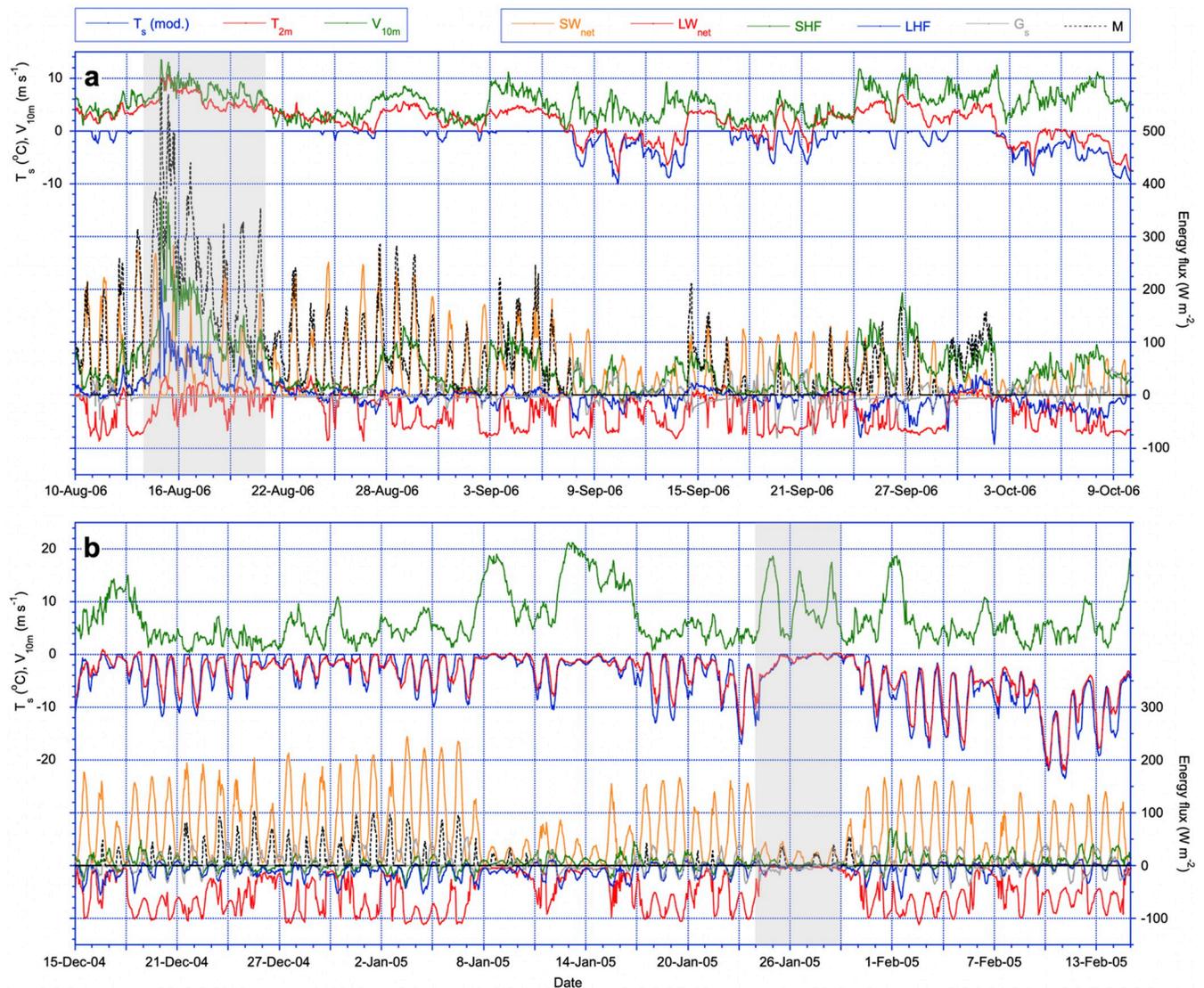
Fig 3. Time series of hourly average near-surface air temperature (T_{2m}), surface temperature (T_s) and 10 m wind speed (V_{10m}) (left axis) and SEB components (right axis) at (a) S5 along the K-transect in the south-western GrIS and (b) at Neumayer station on the Ekström ice shelf, East Antarctic ice sheet. Negative/positive SEB values indicate surface energy losses/gains. Station locations are indicated in Fig 4, images of the measurement sites in Fig 1.

https://doi.org/10.1371/journal.pclm.0000203.g003

increases in dark ice regions with significant glacier ice algae blooms, driven by nutrients from mineral dust [98].

The response of the SEB to clouds and strong winds is very different at Neumayer (Fig 3B). Here, the surface temperature for most of the time remains below freezing and as a result can freely adjust to changes in the energy input. Under windy, cloudy conditions (e.g., 24–28 January 2005, grey band) this results in small surface-to-air temperature and moisture gradients, limiting SHF and LHF. Clouds also limit incoming solar radiation and moreover increase dry snow albedo [99], further reducing SW_{net}. The available energy for melt during cloudy and windy conditions is therefore typically < 50 W m^{-2}, i.e., an order of magnitude smaller than peak melt values reported from the GrIS under similar synoptic conditions. Under clear sky conditions, despite the high surface albedo, the solar energy input is large at daytime ($SW_{net} > 200$ W m^{-2}). In response, T_s rapidly increases without directly reaching the melting point. As a
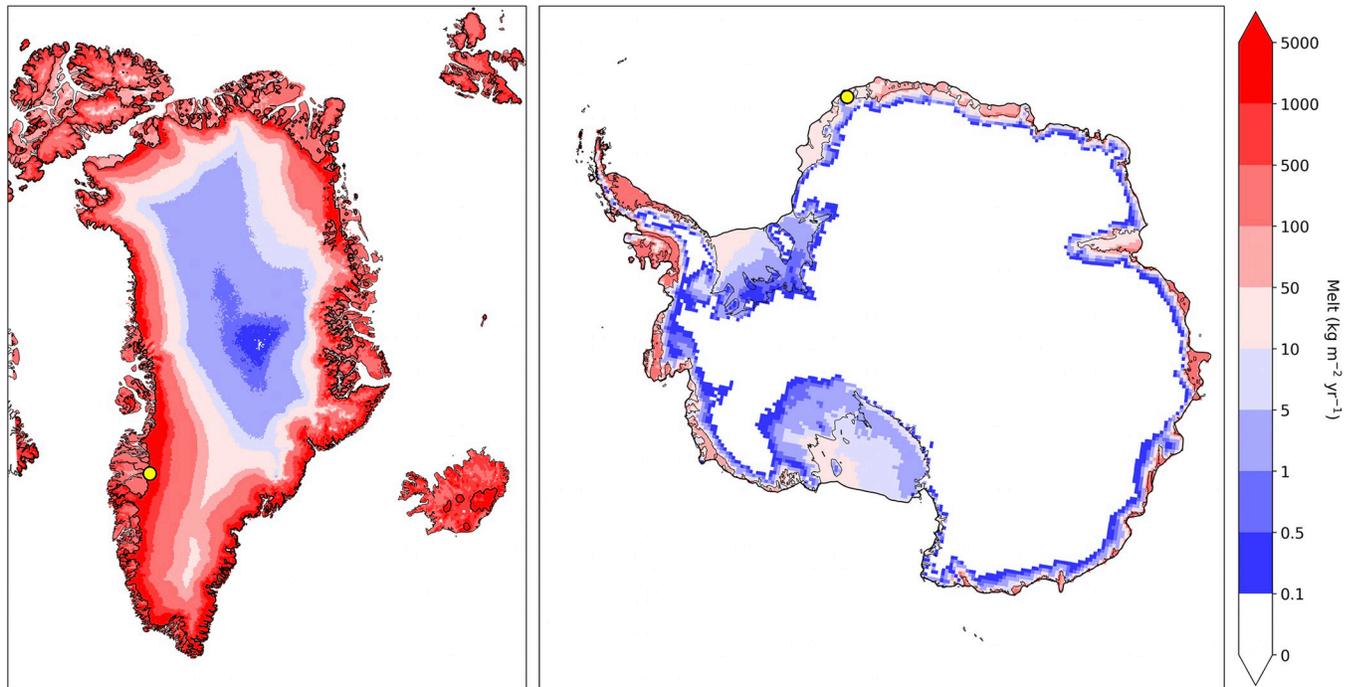
Fig 4. Modelled average (1991–2020) annual melt on the GrIS (left, 0,05 latitudinal degree or ~5.5 km resolution) and the AIS (right, 0.25 latitudinal degree or ~27 km resolution) from the polar regional climate model RACMO2.3p2. Continuous black lines indicate grounded ice sheet margin or coastlines. Yellow dots indicate locations of AWS S5 (Greenland) and Neumayer base (Antarctica). Note the nonlinear melt scale. Made with Natural Earth (Public Domain, https://www.naturalearthdata.com/about/terms-of-use/).

https://doi.org/10.1371/journal.pclm.0000203.g004

result, the surface initially becomes warmer and moister than the near-surface air, leading to weak convection (SHF < 0), sublimation (LHF < 0), a more strongly negative LW_{net} that -in contrast to S5- exhibits a pronounced diurnal cycle, and negative G_s. All these energy sinks efficiently transport the absorbed solar radiation energy away from the surface, limiting melt energy to typically M < 100 W m^{-2}. This still represents a doubling compared to cloudy and windy conditions, and we conclude that in contrast to the GrIS, melt variability in the marginal AIS is mainly driven by variations in absorbed solar radiation, peaking at noon during clear sky conditions.

3.2 Spatial distribution of average melt rate

In situ-derived melt rates from weather stations such as depicted in Fig 3 are far and apart, especially on the AIS, and on both ice sheets the time series are often relatively short and incomplete [24]. As explained in Section 2.3, satellite-derived melt maps are highly valuable to fill in the gaps in space and time. Satellite time series are relatively short, as they often depend on the lifetime of individual satellite missions (typically < 10 years). Moreover, they do not provide information on partitioning of melt energy over the SEB components like models and in situ observations do. Regional climate models are useful to further advance the interpretation, as they produce ice sheet wide melt maps including SEB and surface mass balance components at high temporal (<hourly) and reasonable spatial (2.5–25 km) resolution, enabling the partitioning of mass and energy fluxes [100]. They provide this information for epochs where reliable boundary forcing is available in the form of atmospheric re-analyses, i.e., from 1958 onwards for the GrIS and 1979 onwards for the AIS [33, 101], but they also enable future melt projections. Although considerable uncertainties in model melt products remain (see

Section 2.4), direct comparisons between modelled melt rate from dedicated 'polar' regional models over ice sheets, in-situ observations and satellite data usually show reasonable agreement [33, 92, 94, 101].

As an example, Fig 4 shows GrIS and AIS annual melt maps from the polar regional climate model RACMO2.3p2, forced at the boundaries by European Centre for Medium-range Weather Forecasts (ECMWF) Re-Analysis (ERA5) and averaged for the climatological period 1991–2020 [33, 101]. On the AIS (Fig 4B), modelled melt mainly occurs at lower elevations away from the cold interior. The deepest melt incursions occur up to 1500 m asl in West Antarctica, a result of large scale föhn effects in response to atmospheric river activity and El Niño [102, 103]. On the grounded ice sheet, annual melt is small, typically below 50 kg m^{-2} yr^{-1}. Melt is larger over the low-lying, floating, and northward extending ice shelves, but generally remains below 500 kg m^{-2} yr^{-1}. Over the GrIS, in contrast, melt occasionally occurs even over the highest parts of the interior ice sheet, if large-scale as well as boundary-layer atmospheric conditions are favourable, e.g. during the summer of 2012 [104]. Closer to the margin in the ablation area, for part of the year the surface consists of dark, bare ice, enhancing the absorption of solar radiation. In combination with the peak melt events during strong wind episodes described in Section 3.1, annual melt fluxes can reach up to 5000 kg m^{-2} yr^{-1}, i.e., an order of magnitude larger than the highest values found on the AIS. The positive melt values over ice-free tundra represent the melting of seasonal snow, which is small here owing to the relatively dry regional climate.

3.3 Interannual variability and long-term trends

Fig 5 shows time series of hindcast (i.e., constrained by observations) annual melt (solid lines) integrated over the contiguous GrIS (1958–2021, red squares, 5.5 km resolution) and AIS (including ice shelves, 1979–2021, blue squares, 27 km resolution), using the regional climate model RACMO2.3p2. Melt estimates from satellite data (orange triangles) are from QuikSCAT for the AIS [23] and SSMIS for the GrIS [79]. The agreement with satellite estimates of annual melt is good (r^2 = 0.92 for the GrIS and r^2 = 0.78 for the AIS), with the average bias suggesting a typical uncertainty in the modelled and observed melt flux of ~20%. During the hindcast period, a significant positive trend is found since the mid-1990s for melt on the GrIS, but not for the AIS. The 1991–2020 relative variability (standard deviation divided by the mean) in annual melt is similar for both ice sheets: 0.24 (AIS) and 0.27 (GrIS). For the GrIS, 2012 stands out as an extreme melt year, exceeding the average by more than three standard deviations [104].

The dashed lines in Fig 5 represent RACMO2.3p2 modelled annual melt when forced at the lateral boundaries using the earth system model CESM2. Earth system models are typically not constrained by observations, apart from prescribed greenhouse gas and stratospheric ozone concentrations. Nonetheless, average melt as well as interannual variability over both ice sheets is well simulated for the historical period (up to 2014), as well as the delayed emergence of an increase in AIS melt. This provides confidence in the combination of forcing and dynamical downscaling models for use in future melt projections. After 2015, for the fossil-fuelled development emission scenario SSP5-8.5, a five- (GrIS) to ten-fold (AIS) increase in surface melt is projected towards the end of the century, accompanied by an increase in variability following the rapidly increasing surface area of the melt zone, which more and more often extends to the flat interior ice sheets. In this pessimistic climate scenario, 2012-like melt years are projected to become the norm on the GrIS from 2050 onwards.

4. Conclusions and outlook

The main temporal and spatial characteristics of the surface melt weather and climate of the ice sheets of Greenland (GrIS) and Antarctica (AIS) are presented and contrasted. Essential for
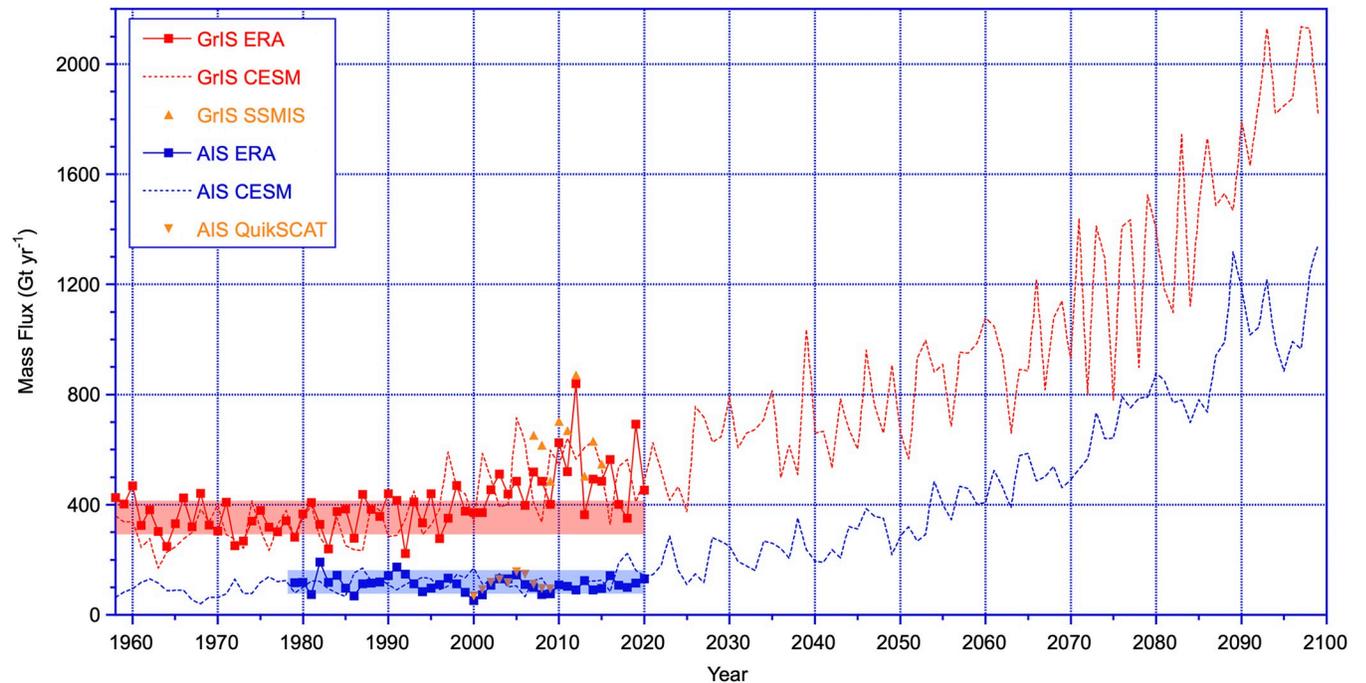
Fig 5. Timeseries of RACMO2.3p2 annual melt totals over the contiguous GrIS (red) and AIS including ice shelves (blue). Solid lines represent hindcast using ERA forcing, dashed lines represent forcing from the earth system model CESM2 for the historical period (up to 2014) and for a high-warming, fossil-fuelled development scenario SSP5-8.5 (until 2100). Orange triangles are satellite-based melt estimates, coloured bands indicate 1961–1990 (GrIS) and 1979–1990 (AIS) range (average +/- one standard deviation).

https://doi.org/10.1371/journal.pclm.0000203.g005

our understanding of the processes driving temporal and spatial variations in ice sheet surface melt are in situ observations from manned and automatic weather stations. When equipped with the proper set of sensors ('SEB-enabled'), these can be used to calculate melt energy. The results reveal important intra- and interdiurnal surface melt variability ('melt weather') as well as different sensitivities of melt rate to synoptic weather systems for both ice sheets.

Because these in-situ observations are scarce, hindcasts using satellites and regional climate models must be used to fill the gaps in space and time and assess the melt 'climate'. These show that melt has increased by ~30% on the GrIS since the mid-1990s, while no obvious melt trend is found for the AIS since 1979, in line with [94]. A recently reached milestone is that historical melt rate, trends and variability on both ice sheets can be well reconstructed using a combination of an unconstrained earth system model with a polar regional climate model. This clears the way for credible projections of future ice sheet surface melt. We present an example for a fossil-fuelled development scenario, which results in a five- (GrIS) to tenfold (AIS) increase in surface melt towards 2100.

In situ SEB observations are invaluable to validate, evaluate, develop, improve, and calibrate satellite- and model-based estimates of ice sheet surface melt. Efforts to expand this observational capability should be prioritised. For the GrIS, the merging in 2021 of the PROMICE (ablation zone) and GC-Net (accumulation zone) AWS networks by the Geological Survey of Denmark and Greenland (GEUS) was an important milestone. A similar effort is needed for the AIS, despite the logistical challenges this presents. An advantage is that in the comparably homogenous surface environment of the ice sheets, these in situ observations are representative for relatively large areas, which makes them compatible with the typical footprint of satellite melt products and grid cells of (regional) climate models. Another important emerging

application is the observation of surface ice sheet melt rate from space, trained by these in situ observations.

For (regional) climate models, the improved availability of in-situ and remotely sensed evaluation data will improve the accuracy of modelled surface melt. For the GrIS, improved agreement with in situ observations is found after statistical downscaling the RCM output to 1 km resolution, better resolving the strong ablation on marginal, low-lying and narrow glacier tongues [105]. A similar improvement with enhanced spatial resolution through dynamical/statistical downscaling is expected for the steeper parts of the AIS, notably the AP [106, 107]. Alternatively, observations can be directly assimilated in (regional) climate models to enable high-resolution, high fidelity re-analysis products specifically targeting the surface mass balance of ice sheets. A recent example is the 2.5 km resolution Copernicus Arctic Regional Reanalysis (CARRA) over Greenland.

In addition to automatic measurements, shorter, dedicated experimental efforts on both ice sheets should address in more detail (near-) surface processes such as the role of ice sheet surface roughness [72], the snowmelt-albedo feedback [108], the impact of bio-albedo [109, 110], drifting snow processes [111] and the role of refreezing and capillary retention in firn to convert melt to runoff [112]. The latter process is important in the upper ice layers, where subsurface melt increases porosity [9, 113], and in the firn layer, which slowly saturates when melt rates increase, potentially leading to an abrupt acceleration of mass loss for both ice sheets [114, 115].

Acknowledgments

Author Contributions

Conceptualization: Michiel R. van den Broeke.

Data curation: Michiel R. van den Broeke, Peter Kuipers Munneke, Brice Noël, Carleen Reijmer, Paul Smeets, Willem Jan van de Berg, J. Melchior van Wessem.

Formal analysis: Michiel R. van den Broeke.

Funding acquisition: Michiel R. van den Broeke.

Investigation: Michiel R. van den Broeke.

Methodology: Michiel R. van den Broeke, Peter Kuipers Munneke, Brice Noël, Carleen Reijmer, Paul Smeets, Willem Jan van de Berg, J. Melchior van Wessem.

Project administration: Michiel R. van den Broeke.

Resources: Michiel R. van den Broeke.

Software: Michiel R. van den Broeke, Peter Kuipers Munneke, Brice Noël, Carleen Reijmer, Paul Smeets, Willem Jan van de Berg, J. Melchior van Wessem.

Supervision: Michiel R. van den Broeke.

Validation: Michiel R. van den Broeke, Peter Kuipers Munneke, Brice Noël, Carleen Reijmer, Paul Smeets, Willem Jan van de Berg, J. Melchior van Wessem.

Visualization: Michiel R. van den Broeke.

Writing – original draft: Michiel R. van den Broeke.

Writing – review & editing: Michiel R. van den Broeke, Peter Kuipers Munneke, Brice Noël, Carleen Reijmer, Paul Smeets, Willem Jan van de Berg, J. Melchior van Wessem.

References

1. IMBIE. Mass balance of the Antarctic Ice Sheet from 1992 to 2017. Nature. 2018; 558(7709):219–22. Epub 20180613. https://doi.org/10.1038/s41586-018-0179-y PMID: 29899482.

2. IMBIE. Mass balance of the Greenland Ice Sheet from 1992 to 2018. Nature. 2020; 579(7798):233–9. Epub 20191210. https://doi.org/10.1038/s41586-019-1855-2 PMID: 31822019.

3. Frederikse T, Landerer F, Caron L, Adhikari S, Parkes D, Humphrey VW, et al. The causes of sea-level rise since 1900. Nature. 2020; 584(7821):393–+. https://doi.org/10.1038/s41586-020-2591-3 WOS:000563935100015. PMID: 32814886

4. Dangendorf S, Hay C, Calafat FM, Marcos M, Piecuch CG, Berk K, et al. Persistent acceleration in global sea-level rise since the 1960s. Nature Climate Change. 2019; 9(9):705–+. https://doi.org/10.1038/s41558-019-0531-8 WOS:000483551700022.

5. Van den Broeke MR, Enderlin EM, Howat IM, Kuipers Munneke P, Noël BPY, Van de Berg WJ, et al. On the recent contribution of the Greenland ice sheet to sea level change. The Cryosphere. 2016; 10 (5):1933–46. https://doi.org/10.5194/tc-10-1933-2016

6. Tedstone AJ, Machguth H. Increasing surface runoff from Greenland's firn areas. Nat Clim Chang. 2022; 12(7):672–6. Epub 20220616. https://doi.org/10.1038/s41558-022-01371-z PMID: 35811787; PubMed Central PMCID: PMC7613031.

7. Noël B, Van de Berg WJ, Lhermitte S, Van den Broeke MR. Rapid ablation zone expansion amplifies north Greenland mass loss. Science Advances. 2019; 5(9). https://doi.org/10.1126/sciadv.aaw0123 WOS:000491128800002. PMID: 31517042

8. Smith LC, Yang K, Pitcher LH, Overstreet BT, Chu VW, Rennermalm AK, et al. Direct measurements of meltwater runoff on the Greenland ice sheet surface. Proc Natl Acad Sci U S A. 2017; 114(50): E10622–E31. Epub 2017/12/07. https://doi.org/10.1073/pnas.1707743114 PMID: 29208716; PubMed Central PMCID: PMC5740616.

9. Cooper MG, Smith LC, Rennermalm AK, Miège C, Pitcher LH, Ryan JC, et al. Meltwater storage in low-density near-surface bare ice in the Greenland ice sheet ablation zone. The Cryosphere. 2018; 12 (3):955–70. https://doi.org/10.5194/tc-12-955-2018

10. Kuipers Munneke P, Smeets CJPP, Reijmer CH, Oerlemans J, van de Wal RSW, van den Broeke MR. The K-transect on the western Greenland Ice Sheet: Surface energy balance (2003–2016). Arctic, Antarctic, and Alpine Research. 2018; 50(1). https://doi.org/10.1080/15230430.2017.1420952

11. Zwally HJ, Abdalati W, Herring T, Larson K, Saba J, Steffen K. Surface melt-induced acceleration of Greenland ice sheet flow. Science. 2002; 297:218–22. https://doi.org/10.1126/science.1072708 PMID: 12052902

12. Shannon SR, Payne AJ, Bartholomew ID, van den Broeke MR, Edwards TL, Fettweis X, et al. Enhanced basal lubrication and the contribution of the Greenland ice sheet to future sea-level rise. Proc Natl Acad Sci U S A. 2013; 110(35):14156–61. Epub 2013/08/14. https://doi.org/10.1073/pnas.1212647110 PMID: 23940337; PubMed Central PMCID: PMC3761614.

13. Van de Wal RS, Boot W, Van den Broeke MR, Smeets CJ, Reijmer CH, Donker JJ, et al. Large and rapid melt-induced velocity changes in the ablation zone of the Greenland Ice Sheet. Science. 2008; 321(5885):111–3. Epub 2008/07/05. https://doi.org/10.1126/science.1158540 PMID: 18599784.

14. Phillips T, Rajaram H, Colgan W, Steffen K, Abdalati W. Evaluation of cryo-hydrologic warming as an explanation for increased ice velocities in the wet snow zone, Sermeq Avannarleq, West Greenland. Journal of Geophysical Research-Earth Surface. 2013; 118(3):1241–56. https://doi.org/10.1002/jgrf.20079 WOS:000325978500004.

15. Slater DA, Straneo F. Submarine melting of glaciers in Greenland amplified by atmospheric warming. Nature Geoscience. 2022; 15(10):794–9. https://doi.org/10.1038/s41561-022-01035-9

16. Jenkins A. A Simple Model of the Ice Shelf–Ocean Boundary Layer and Current. Journal of Physical Oceanography. 2016; 46(6):1785–803. https://doi.org/10.1175/jpo-d-15-0194.1

17. King MD, Howat IM, Jeong S, Noh MJ, Wouters B, Noel B, et al. Seasonal to decadal variability in ice discharge from the Greenland Ice Sheet. Cryosphere. 2018; 12(12):3813–25. Epub 20181203. https://doi.org/10.5194/tc-12-3813-2018 PMID: 31217911; PubMed Central PMCID: PMC6582977.

18. Mouginot J, Rignot E, Bjork AA, van den Broeke M, Millan R, Morlighem M, et al. Forty-six years of Greenland Ice Sheet mass balance from 1972 to 2018. Proc Natl Acad Sci U S A. 2019; 116

(19):9239–44. Epub 20190422. https://doi.org/10.1073/pnas.1904242116 PMID: 31010924; PubMed Central PMCID: PMC6511040.

19. Smeets PCJP, Kuipers Munneke P, van As D, van den Broeke MR, Boot W, Oerlemans H, et al. The K-transect in west Greenland: Automatic weather station data (1993–2016). Arctic, Antarctic, and Alpine Research. 2018; 50(1). https://doi.org/10.1080/15230430.2017.1420954

20. König-Langlo G, Loose B. The Meteorological Observatory at Neumayer Stations (GvN and NM-II) Antarctica. Polarforschung. 2006; 76 (1–2):25–38. https://doi.org/10.2312/polarforschung.76.1–2.25

21. Lhermitte S, Sun S, Shuman C, Wouters B, Pattyn F, Wuite J, et al. Damage accelerates ice shelf instability and mass loss in Amundsen Sea Embayment. Proc Natl Acad Sci U S A. 2020; 117 (40):24735–41. Epub 20200914. https://doi.org/10.1073/pnas.1912890117 PMID: 32929004; PubMed Central PMCID: PMC7547219.

22. Rignot E, Mouginot J, Scheuchl B, van den Broeke M, van Wessem MJ, Morlighem M. Four decades of Antarctic Ice Sheet mass balance from 1979–2017. Proc Natl Acad Sci U S A. 2019; 116(4):1095–103. Epub 20190114. https://doi.org/10.1073/pnas.1812883116 PMID: 30642972; PubMed Central PMCID: PMC6347714.

23. Trusel LD, Frey KE, Das SB, Munneke PK, van den Broeke MR. Satellite-based estimates of Antarctic surface meltwater fluxes. Geophysical Research Letters. 2013; 40(23):6148–53. https://doi.org/10.1002/2013gl058138

24. Jakobs CL, Reijmer CH, Smeets CJPP, Trusel LD, van de Berg WJ, van den Broeke MR, et al. A benchmark dataset of in situ Antarctic surface melt rates and energy balance. Journal of Glaciology. 2020; 66(256):291–302. https://doi.org/10.1017/jog.2020.6

25. Ligtenberg SRM, Lenaerts JTM, Van den Broeke MR, Scambos TA. On the formation of blue ice on Byrd Glacier, Antarctica. Journal of Glaciology. 2014; 60(219):41–50. https://doi.org/10.3189/2014JoG13J116

26. Hu Z, Kuipers Munneke P, Lhermitte S, Dirscherl M, Ji C, van den Broeke M. FABIAN: A daily product of Fractional Austral-summer Blue Ice over ANtarctica during 2000–2021 based on MODIS imagery using Google Earth Engine. Remote Sensing of Environment. 2022; 280. https://doi.org/10.1016/j.rse.2022.113202

27. Tollenaar V, Zekollari H, Lhermitte S, Tax DMJ, Debaille V, Goderis S, et al. Unexplored Antarctic meteorite collection sites revealed through machine learning. Science Advances. 2022; 8(4). https://doi.org/10.1126/sciadv.abj8138 WOS:000747329300010. PMID: 35080966

28. Winther J-G, Jespersen MN, Liston GE. Blue-ice areas in Antarctica derived from NOAA AVHRR satellite data. Journal of Glaciology. 2001; 47(157):325–34. https://doi.org/10.3189/172756501781832386

29. Lenaerts JTM, Lhermitte S, Drews R, Ligtenberg SRM, Berger S, Helm V, et al. Meltwater produced by wind–albedo interaction stored in an East Antarctic ice shelf. Nature Climate Change. 2016; 7 (1):58–62. https://doi.org/10.1038/nclimate3180

30. Bintanja R. On the glaciological, meteorological, and climatological significance of Antarctic blue ice areas. Reviews of Geophysics. 1999; 37(3):337–59. https://doi.org/10.1029/1999rg900007

31. Van den Broeke M. Depth and Density of the Antarctic Firn Layer. Arctic, Antarctic, and Alpine Research. 2008; 40(2):432–8. https://doi.org/10.1657/1523-0430(07–021)[broeke]2.0.Co;2.

32. Jakobs CL, Reijmer CH, Kuipers Munneke P, König-Langlo G, van den Broeke MR. Quantifying the snowmelt–albedo feedback at Neumayer Station, East Antarctica. The Cryosphere. 2019; 13 (5):1473–85. https://doi.org/10.5194/tc-13-1473-2019

33. Van Wessem JM, Van de Berg WJ, Noël BPY, van Meijgaard E, Amory C, Birnbaum G, et al. Modelling the climate and surface mass balance of polar ice sheets using RACMO2 –Part 2: Antarctica (1979–2016). The Cryosphere. 2018; 12(4):1479–98. https://doi.org/10.5194/tc-12-1479-2018

34. Scambos TA, Hulbe C, Fahnestock M, Bohlander J. The link between climate warming and break-up of ice shelves in the Antarctic Peninsula. Journal of Glaciology. 2000; 46(154):516–30. https://doi.org/10.3189/172756500781833043 WOS:000165920700018.

35. Kuipers Munneke P, Ligtenberg SRM, van den Broeke MR, Vaughan DG. Firn air depletion as a precursor of Antarctic ice-shelf collapse. Journal of Glaciology. 2014; 60(220):205–14. https://doi.org/10.3189/2014JoG13J183 WOS:000336198100001.

36. Banwell AF, Willis IC, Macdonald GJ, Goodsell B, MacAyeal DR. Direct measurements of ice-shelf flexure caused by surface meltwater ponding and drainage. Nature Communications. 2019;10. https://doi.org/10.1038/s41467-019-08522-5 WOS:000458567500010. PMID: 30760715

37. Laffin MK, Zender CS, van Wessem M, Marinsek S. The role of föhn winds in eastern Antarctic Peninsula rapid ice shelf collapse. The Cryosphere. 2022; 16(4):1369–81. https://doi.org/10.5194/tc-16-1369-2022

38. Arthur JF, Stokes CR, Jamieson SSR, Miles BWJ, Carr JR, Leeson AA. The triggers of the disaggregation of Voyeykov Ice Shelf (2007), Wilkes Land, East Antarctica, and its subsequent evolution. Journal of Glaciology. 2021; 67(265):933–51. https://doi.org/10.1017/jog.2021.45

39. Scambos T, Fricker HA, Liu C-C, Bohlander J, Fastook J, Sargent A, et al. Ice shelf disintegration by plate bending and hydro-fracture: Satellite observations and model results of the 2008 Wilkins ice shelf break-ups. Earth and Planetary Science Letters. 2009; 280(1–4):51–60. https://doi.org/10.1016/j.epsl.2008.12.027

40. Wille JD, Favier V, Jourdain NC, Kittel C, Turton JV, Agosta C, et al. Intense atmospheric rivers can weaken ice shelf stability at the Antarctic Peninsula. Communications Earth & Environment. 2022; 3 (1). https://doi.org/10.1038/s43247-022-00422-9

41. Fürst JJ, Durand G, Gillet-Chaulet F, Tavard L, Rankl M, Braun M, et al. The safety band of Antarctic ice shelves. Nature Climate Change. 2016; 6(5):479–82. https://doi.org/10.1038/nclimate2912

42. Lai CY, Kingslake J, Wearing MG, Chen PC, Gentine P, Li H, et al. Vulnerability of Antarctica's ice shelves to meltwater-driven fracture. Nature. 2020; 584(7822):574–8. Epub 20200826. https://doi.org/10.1038/s41586-020-2627-8 PMID: 32848224.

43. Reese R, Gudmundsson GH, Levermann A, Winkelmann R. The far reach of ice-shelf thinning in Antarctica. Nature Climate Change. 2018; 8(1):53–7. https://doi.org/10.1038/s41558-017-0020-x

44. Rott H, Skvarca P, Nagler T. Rapid collapse of northern Larsen Ice Shelf, Antarctica. Science. 1996; 271(5250):788–92. https://doi.org/10.1126/science.271.5250.788 WOS:A1996TU69400040.

45. Scambos TA, Bohlander JA, Shuman CA, Skvarca P. Glacier acceleration and thinning after ice shelf collapse in the Larsen B embayment, Antarctica. Geophysical Research Letters. 2004; 31(18). https://doi.org/10.1029/2004gl020670 WOS:000224125900002.

46. Leeson AA, Forster E, Rice A, Gourmelen N, Wessem JM. Evolution of Supraglacial Lakes on the Larsen B Ice Shelf in the Decades Before it Collapsed. Geophysical Research Letters. 2020; 47(4). https://doi.org/10.1029/2019gl085591

47. Trusel LD, Frey KE, Das SB, Karnauskas KB, Kuipers Munneke P, van Meijgaard E, et al. Divergent trajectories of Antarctic surface melt under two twenty-first-century climate scenarios. Nature Geoscience. 2015; 8(12):927–32. https://doi.org/10.1038/ngeo2563

48. DeConto RM, Pollard D. Contribution of Antarctica to past and future sea-level rise. Nature. 2016; 531 (7596):591–7. https://doi.org/10.1038/nature17145 PMID: 27029274.

49. Forster RR, Box JE, van den Broeke MR, Miege C, Burgess EW, van Angelen JH, et al. Extensive liquid meltwater storage in firn within the Greenland ice sheet. Nature Geoscience. 2014; 7(2):95–8. https://doi.org/10.1038/NGEO2043 WOS:000331140800011.

50. Miller JZ, Culberg R, Long DG, Shuman CA, Schroeder DM, Brodzik MJ. An empirical algorithm to map perennial firn aquifers and ice slabs within the Greenland Ice Sheet using satellite L-band microwave radiometry. The Cryosphere. 2022; 16(1):103–25. https://doi.org/10.5194/tc-16-103-2022

51. Buth LG, Wouters B, Veldhuijsen SBM, Lhermitte S, Kuipers Munneke P, van den Broeke MR. Sentinel-1 detection of seasonal and perennial firn aquifers in the Antarctic Peninsula. Cryosphere Discussions. 2022. https://doi.org/10.5194/tc-2022-127

52. Van Wessem JM, Steger CR, Wever N, Van den Broeke MR. An exploratory modelling study of perennial firn aquifers in the Antarctic Peninsula for the period 1979–2016. The Cryosphere. 2021; 15 (2):695–714. https://doi.org/10.5194/tc-15-695-2021

53. MacDonell S, Fernandoy F, Villar P, Hammann A. Stratigraphic Analysis of Firn Cores from an Antarctic Ice Shelf Firn Aquifer. Water. 2021; 13(5). https://doi.org/10.3390/w13050731

54. Montgomery L, Miège C, Miller J, Scambos TA, Wallin B, Miller O, et al. Hydrologic Properties of a Highly Permeable Firn Aquifer in the Wilkins Ice Shelf, Antarctica. Geophysical Research Letters. 2020; 47(22). https://doi.org/10.1029/2020gl089552

55. Horlings AN, Christianson K, Miège C. Expansion of Firn Aquifers in Southeast Greenland. Journal of Geophysical Research: Earth Surface. 2022; 127(10). https://doi.org/10.1029/2022jf006753

56. Poinar K, Dow CF, Andrews LC. Long-Term Support of an Active Subglacial Hydrologic System in Southeast Greenland by Firn Aquifers. Geophysical Research Letters. 2019; 46(9):4772–81. https://doi.org/10.1029/2019gl082786

57. Mankoff KD, Fettweis X, Langen PL, Stendel M, Kjeldsen KK, Karlsson NB, et al. Greenland ice sheet mass balance from 1840 through next week. Earth System Science Data. 2021; 13(10):5001–25. https://doi.org/10.5194/essd-13-5001-2021

58. Niwano M, Box JE, Wehrlé A, Vandecrux B, Colgan WT, Cappelen J. Rainfall on the Greenland Ice Sheet: Present-Day Climatology From a High-Resolution Non-Hydrostatic Polar Regional Climate Model. Geophysical Research Letters. 2021; 48(15). https://doi.org/10.1029/2021gl092942

59. Box JE, Wehrlé A, van As D, Fausto RS, Kjeldsen KK, Dachauer A, et al. Greenland Ice Sheet Rainfall, Heat and Albedo Feedback Impacts From the Mid-August 2021 Atmospheric River. Geophysical Research Letters. 2022; 49(11). https://doi.org/10.1029/2021gl097356

60. Huai B, van den Broeke MR, Reijmer CH, Noël B. A Daily 1-km Resolution Greenland Rainfall Climatology (1958–2020) From Statistical Downscaling of a Regional Atmospheric Climate Model. Journal of Geophysical Research: Atmospheres. 2022; 127(17). https://doi.org/10.1029/2022jd036688

61. Vignon É, Roussel ML, Gorodetskaya IV, Genthon C, Berne A. Present and Future of Rainfall in Antarctica. Geophysical Research Letters. 2021; 48(8). https://doi.org/10.1029/2020gl092281

62. Kuipers Munneke P, van den Broeke MR, King JC, Gray T, Reijmer CH. Near-surface climate and surface energy budget of Larsen C ice shelf, Antarctic Peninsula. The Cryosphere. 2012; 6(2):353–63. https://doi.org/10.5194/tc-6-353-2012

63. Van den Broeke MR, Smeets P, Ettema J, Van der Veen C, Van de Wal R, Oerlemans J. Partitioning of melt energy and meltwater fluxes in the ablation zone of the west Greenland ice sheet. Cryosphere. 2008; 2(2):179–89. https://doi.org/10.5194/tc-2-179-2008 WOS:000207505200009.

64. Cogley JG, Hock R, Rasmussen LA, Arendt AA, Bauder A, Jansson P, et al. Glossary of glacier mass balance and related terms. HP-VII Technical Documents in Hydrology No 86, IACS Contribution No 2, UNESCO-IHP, Paris. 2011. https://doi.org/10.5167/uzh-53475

65. Lenaerts JTM, Medley B, van den Broeke MR, Wouters B. Observing and Modeling Ice Sheet Surface Mass Balance. Reviews of Geophysics. 2019; 57(2):376–420. https://doi.org/10.1029/2018RG000622 PMID: 31598609

66. Fausto RS, van As D, Mankoff KD, Vandecrux B, Citterio M, Ahlstrøm AP, et al. Programme for Monitoring of the Greenland Ice Sheet (PROMICE) automatic weather station data. Earth System Science Data. 2021; 13(8):3819–45. https://doi.org/10.5194/essd-13-3819-2021

67. Steffen K, Box JE. Surface climatology of the Greenland Ice Sheet: Greenland Climate Network 1995–1999. Journal of Geophysical Research Atmospheres. 2001;106. https://doi.org/10.1029/2001JD900161

68. Wang Y, Zhang X, Ning W, Lazzara MA, Ding M, Reijmer CH, et al. The AntAWS dataset: a compilation of Antarctic automatic weather station observations. Earth System Science Data Discussions. 2023. https://doi.org/10.5194/essd-2022-241

69. Van den Broeke MR, König-Langlo G, Picard G, Kuipers Munneke P, Lenaerts J. Surface energy balance, melt and sublimation at Neumayer Station, East Antarctica. Antarctic Science. 2009; 22(01). https://doi.org/10.1017/s0954102009990538

70. Van den Broeke MR, Van As D, Reijmer C, Van de Wal R. Assessing and improving the quality of unattended radiation observations in Antarctica. Journal of Atmospheric and Oceanic Technology. 2004; 21(9):1417–31. https://doi.org/10.1175/1520-0426(2004)021<1417:AAITQO>2.0.CO;2. WOS:000223685100008.

71. Wang W, Zender CS, van As D, Smeets PCJP, van den Broeke MR. A Retrospective, Iterative, Geometry-Based (RIGB) tilt-correction method for radiation observed by automatic weather stations on snow-covered surfaces: application to Greenland. The Cryosphere. 2016; 10(2):727–41. https://doi.org/10.5194/tc-10-727-2016

72. van Tiggelen M, Smeets PCJP, Reijmer CH, van den Broeke MR, van As D, Box JE, et al. Observed and Parameterized Roughness Lengths for Momentum and Heat Over Rough Ice Surfaces. Journal of Geophysical Research: Atmospheres. 2023; 128(2). https://doi.org/10.1029/2022jd036970

73. Smeets CJPP, van den Broeke MR. Temporal and Spatial Variations of the Aerodynamic Roughness Length in the Ablation Zone of the Greenland Ice Sheet. Boundary-Layer Meteorology. 2008; 128 (3):315–38. https://doi.org/10.1007/s10546-008-9291-0

74. Van Tiggelen M, Smeets PCJP, Reijmer CH, Wouters B, Steiner JF, Nieuwstraten EJ, et al. Mapping the aerodynamic roughness of the Greenland Ice Sheet surface using ICESat-2: evaluation over the K-transect. The Cryosphere. 2021; 15(6):2601–21. https://doi.org/10.5194/tc-15-2601-2021

75. Amory C, Naaim-Bouvet F, Gallee H, Vignon E. Brief communication: Two well-marked cases of aerodynamic adjustment of sastrugi. Cryosphere. 2016; 10(2):743–50. https://doi.org/10.5194/tc-10-743-2016 WOS:000379411800018.

76. Van den Broeke MR, Smeets CJPP, Van de Wal RSW. The seasonal cycle and interannual variability of surface energy balance and melt in the ablation zone of the west Greenland ice sheet. The Cryosphere. 2011; 5(2):377–90. https://doi.org/10.5194/tc-5-377-2011

77. Van den Broeke M, Reijmer C, Van As D, De Wal RV, Oerlemans J, Hamilton G. Seasonal cycles of Antarctic surface energy balance from automatic weather stations. Annals of Glaciology, Vol 41, 2005. 2005; 41:131–9. https://doi.org/10.3189/172756405781813168 WOS:000238029800019.

78. Covi F, Hock R, Reijmer CH. Challenges in modeling the energy balance and melt in the percolation zone of the Greenland ice sheet. Journal of Glaciology. 2022:1–15. https://doi.org/10.1017/jog.2022.54

79. Zheng L, Cheng X, Shang X, Chen Z, Liang Q, Wang K. Greenland Ice Sheet Daily Surface Melt Flux Observed From Space. Geophysical Research Letters. 2022; 49(6). https://doi.org/10.1029/2021gl096690

80. Slater T, Shepherd A, McMillan M, Leeson A, Gilbert L, Muir A, et al. Increased variability in Greenland Ice Sheet runoff from satellite observations. Nature Communications. 2021; 12. https://doi.org/10.1038/s41467-021-26229-4 PMID: 34725324

81. Houtz D, Mätzler C, Naderpour R, Schwank M, Steffen K. Quantifying Surface Melt and Liquid Water on the Greenland Ice Sheet using L-band Radiometry. Remote Sensing of Environment. 2021; 256. https://doi.org/10.1016/j.rse.2021.112341

82. Trusel LD, Frey KE, Das SB. Antarctic surface melting dynamics: Enhanced perspectives from radar scatterometer data. Journal of Geophysical Research: Earth Surface. 2012; 117(F2). https://doi.org/10.1029/2011jf002126

83. De Roda Husman S, Hu Z, Wouters B, Kuipers Munneke P, Veldhuijsen S, Lhermitte S. Remote Sensing of Surface Melt on Antarctica: Opportunities and Challenges. IEEE Journal of Selected Topics in Applied Earth Observations and Remote Sensing 2022. https://doi.org/10.1109/JSTARS.2022.3216953

84. Danabasoglu G, Lamarque JF, Bacmeister J, Bailey DA, DuVivier AK, Edwards J, et al. The Community Earth System Model Version 2 (CESM2). Journal of Advances in Modeling Earth Systems. 2020; 12(2). https://doi.org/10.1029/2019ms001916

85. Van Kampenhout L, Rhoades AM, Herrington AR, Zarzycki CM, Lenaerts JTM, Sacks WJ, et al. Regional grid refinement in an Earth system model: impacts on the simulated Greenland surface mass balance. The Cryosphere. 2019; 13(6):1547–64. https://doi.org/10.5194/tc-13-1547-2019

86. Van Kampenhout L, Lenaerts JTM, Lipscomb WH, Sacks WJ, Lawrence DM, Slater AG, et al. Improving the Representation of Polar Snow and Firn in the Community Earth System Model. Journal of Advances in Modeling Earth Systems. 2017; 9(7):2583–600. https://doi.org/10.1002/2017ms000988

87. Flanner MG, Zender CS. Linking snowpack microphysics and albedo evolution. Journal of Geophysical Research. 2006; 111(D12). https://doi.org/10.1029/2005jd006834

88. Lawrence DM, Fisher RA, Koven CD, Oleson KW, Swenson SC, Bonan G, et al. The Community Land Model Version 5: Description of New Features, Benchmarking, and Impact of Forcing Uncertainty. Journal of Advances in Modeling Earth Systems. 2019; 11(12):4245–87. https://doi.org/10.1029/2018ms001583

89. Van Kampenhout L, Lenaerts JTM, Lipscomb WH, Lhermitte S, Noël B, Vizcaíno M, et al. Present-Day Greenland Ice Sheet Climate and Surface Mass Balance in CESM2. Journal of Geophysical Research: Earth Surface. 2020; 125(2). https://doi.org/10.1029/2019jf005318

90. Lenaerts JTM, Vizcaino M, Fyke J, Van Kampenhout L, Van den Broeke MR. Present-day and future Antarctic ice sheet climate and surface mass balance in the Community Earth System Model. Climate Dynamics. 2016; 47(5–6):1367–81. https://doi.org/10.1007/s00382-015-2907-4

91. Dunmire D, Lenaerts JTM, Datta RT, Gorte T. Antarctic surface climate and surface mass balance in the Community Earth System Model version 2 during the satellite era and into the future (1979–2100). The Cryosphere. 2022; 16(10):4163–84. https://doi.org/10.5194/tc-16-4163-2022

92. Fettweis X, Hofer S, Krebs-Kanzow U, Amory C, Aoki T, Berends CJ, et al. GrSMBMIP: intercomparison of the modelled 1980–2012 surface mass balance over the Greenland Ice Sheet. The Cryosphere. 2020; 14(11):3935–58. https://doi.org/10.5194/tc-14-3935-2020

93. Hansen N, Langen PL, Boberg F, Forsberg R, Simonsen SB, Thejll P, et al. Downscaled surface mass balance in Antarctica: impacts of subsurface processes and large-scale atmospheric circulation. The Cryosphere. 2021; 15(9):4315–33. https://doi.org/10.5194/tc-15-4315-2021

94. Kuipers Munneke P, Picard G, van den Broeke MR, Lenaerts JTM, van Meijgaard E. Insignificant change in Antarctic snowmelt volume since 1979. Geophysical Research Letters. 2012; 39(1):n/a-n/a. https://doi.org/10.1029/2011gl050207

95. Agosta C, Amory C, Kittel C, Orsi A, Favier V, Gallée H, et al. Estimation of the Antarctic surface mass balance using the regional climate model MAR (1979–2015) and identification of dominant processes. The Cryosphere. 2019; 13(1):281–96. https://doi.org/10.5194/tc-13-281-2019

96. Carter J, Leeson A, Orr A, Kittel C, van Wessem JM. Variability in Antarctic surface climatology across regional climate models and reanalysis datasets. The Cryosphere. 2022; 16(9):3815–41. https://doi.org/10.5194/tc-16-3815-2022

97. Van den Broeke MR, Gallée H. Observation and simulation of barrier winds at the western margin of the Greenland ice sheet. Quarterly Journal of the Royal Meteorological Society. 1996; 122 (534):1365–83. https://doi.org/10.1256/smsqj.53406 WOS:A1996VF70700006.

98. McCutcheon J, Lutz S, Williamson C, Cook JM, Tedstone AJ, Vanderstraeten A, et al. Mineral phosphorus drives glacier algal blooms on the Greenland Ice Sheet. Nat Commun. 2021; 12(1):570. Epub 20210125. https://doi.org/10.1038/s41467-020-20627-w PMID: 33495440; PubMed Central PMCID: PMC7835244.

99. Wiscombe WJ, Warren SG. A Model for the Spectral Albedo of Snow. I: Pure Snow. Journal of the Atmospheric Sciences. 1980; 37(12):2712–33. https://doi.org/10.1175/1520-0469

100. Van den Broeke MR, Bamber J, Ettema J, Rignot E, Schrama E, Van de Berg WJ, et al. Partitioning recent Greenland mass loss. Science. 2009; 326(5955):984–6. Epub 2009/12/08. https://doi.org/10.1126/science.1178176 PMID: 19965509.

101. Noël B, van de Berg WJ, van Wessem JM, van Meijgaard E, van As D, Lenaerts JTM, et al. Modelling the climate and surface mass balance of polar ice sheets using RACMO2 –Part 1: Greenland (1958–2016). The Cryosphere. 2018; 12(3):811–31. https://doi.org/10.5194/tc-12-811-2018

102. Wille JD, Favier V, Dufour A, Gorodetskaya IV, Turner J, Agosta C, et al. West Antarctic surface melt triggered by atmospheric rivers. Nature Geoscience. 2019; 12(11):911–+. https://doi.org/10.1038/s41561-019-0460-1 WOS:000493905700012.

103. Nicolas JP, Vogelmann AM, Scott RC, Wilson AB, Cadeddu MP, Bromwich DH, et al. January 2016 extensive summer melt in West Antarctica favoured by strong El Nino. Nature Communications. 2017; 8. https://doi.org/10.1038/ncomms15799 WOS:000403316800001. PMID: 28643801

104. Bennartz R, Shupe MD, Turner DD, Walden VP, Steffen K, Cox CJ, et al. July 2012 Greenland melt extent enhanced by low-level liquid clouds. Nature. 2013; 496(7443):83–6. https://doi.org/10.1038/nature12002 WOS:000316993400029. PMID: 23552947

105. Noël B, van de Berg WJ, Machguth H, Lhermitte S, Howat I, Fettweis X, et al. A daily, 1 km resolution data set of downscaled Greenland ice sheet surface mass balance (1958–2015). The Cryosphere. 2016; 10(5):2361–77. https://doi.org/10.5194/tc-10-2361-2016

106. van Wessem JM, Ligtenberg SRM, Reijmer CH, van de Berg WJ, van den Broeke MR, Barrand NE, et al. The modelled surface mass balance of the Antarctic Peninsula at 5.5 km horizontal resolution. The Cryosphere. 2016; 10(1):271–85. https://doi.org/10.5194/tc-10-271-2016

107. Lenaerts JTM, Van Den Broeke MR, Scarchilli C, Agosta C. Impact of model resolution on simulated wind, drifting snow and surface mass balance in Terre Adélie, East Antarctica. Journal of Glaciology. 2012; 58(211):821–9. https://doi.org/10.3189/2012JoG12J020

108. Jakobs CL, Reijmer CH, van den Broeke MR, van de Berg WJ, van Wessem JM. Spatial Variability of the Snowmelt-Albedo Feedback in Antarctica. Journal of Geophysical Research: Earth Surface. 2021; 126(2). https://doi.org/10.1029/2020jf005696

109. Stibal M, Box JE, Cameron KA, Langen PL, Yallop ML, Mottram RH, et al. Algae Drive Enhanced Darkening of Bare Ice on the Greenland Ice Sheet. Geophysical Research Letters. 2017; 44 (22):11,463–11,71. https://doi.org/10.1002/2017gl075958

110. Cook JM, Tedstone AJ, Williamson C, McCutcheon J, Hodson AJ, Dayal A, et al. Glacier algae accelerate melt rates on the south-western Greenland Ice Sheet. The Cryosphere. 2020; 14(1):309–30. https://doi.org/10.5194/tc-14-309-2020

111. Amory C. Drifting-snow statistics from multiple-year autonomous measurements in Adélie Land, East Antarctica. The Cryosphere. 2020; 14(5):1713–25. https://doi.org/10.5194/tc-14-1713-2020

112. Machguth H, MacFerrin M, van As D, Box JE, Charalampidis C, Colgan W, et al. Greenland meltwater storage in firn limited by near-surface ice formation. Nature Climate Change. 2016; 6(4):390–3. https://doi.org/10.1038/nclimate2899

113. Rennermalm AK, Smith LC, Chu VW, Box JE, Forster RR, Van den Broeke MR, et al. Evidence of meltwater retention within the Greenland ice sheet. The Cryosphere. 2013; 7(5):1433–45. https://doi.org/10.5194/tc-7-1433-2013

114. van Wessem JM, van den Broeke MR, Wouters B, Lhermitte S. Variable temperature thresholds of melt pond formation on Antarctic ice shelves. Nature Climate Change. 2023. https://doi.org/10.1038/s41558-022-01577-1

115. Noël B, Lenaerts JTM, Lipscomb WH, Thayer-Calder K, van den Broeke MR. Peak refreezing in the Greenland firn layer under future warming scenarios. Nat Commun. 2022; 13(1):6870. Epub 20221111. https://doi.org/10.1038/s41467-022-34524-x PMID: 36369265; PubMed Central PMCID: PMC9652464.